Metals and Materials International (2021) 27:744–752
https://doi.org/10.1007/s12540-020-00673-1

Mechanical, Wear and Thermal Behaviors of Graphene Reinforced Titanium Composites

Mevlüt Gürbüz[1] · Tuğba Mutuk[2] · Pınar Uyan[3,4]

Received: 26 November 2019 / Accepted: 29 January 2020 / Published online: 18 March 2020

Abstract
In this study, the effects of graphene content (0.15, 0.30, 0.45 and 0.60 wt%) on the mechanical, tribological and thermal properties of titanium matrix composites were investigated. The experimental results showed that the highest ultimate compressive strength (845 MPa), tensile strength (613 MPa), lowest mass loss (0.6 mg for 10 N), and lowest wear rate ($WR = 286 \times 10^{-5}$ mm^3/Nm for10 N) were obtained for Ti-0.15GNPs compared with pure titanium (652 MPa, 413 MPa, 1 mg and 5×10^{-5} mm^3/Nm, respectively). The wear rate of composites deteriorates with increasing applied load. From the thermal analysis results, the best thermal conductivity (16 W/mK) and diffusivity (7.1 mm^2/s) were performed for Ti-0.30GNPs composites at room temperature. The thermal behavior of the composites was decreased with increasing graphene content and temperature. It concluded that graphene is an effective reinforcement to develop the mechanical, wear and thermal behavior of titanium matrix composites.

Keywords Composite · Graphene · Mechanical · Thermal · Titanium · Wear

1 Introduction

Titanium (Ti) and its alloys are extensively used in aerospace, aviation, automotive and biomaterial industry. Development of the mechanical properties, thermal conductivities and wear properties are essential in these areas [1–4]. In last decade, the researchers have many efforts to fabricate composite form of Ti reinforced with some ceramics as ZrB_2, SiC, Al_2O_3, TiC, TiB_2, Si_3N_4 etc. [5, 6]. However, these ceramic particulates are not enough to develop the given properties. Thus, some new approaches are needed to enhance the Ti composites properties. In recent years, graphene nanoplatelets (GNPs) are the most popular in advanced materials applications due to its superior mechanical, electrical, thermal and tribological behaviors [7, 8]. Graphene was discovered in 2004 and is being used in many industry areas such as biomedical, computer technology, aerospace, sensing etc. It is a two-dimensional structure of carbon allotrope and the carbon–carbon bond length in graphene is 1.420 Å. The strong carbon bonds give it very good mechanical strength, electrical and thermal conductivity [9–12]. The elastic modulus and tensile properties were reported as 1.0 TPa and 130 GPa, respectively [13].

Recently, graphene has been preferred as reinforcement element in aluminum and magnesium metal matrices to improve the properties of composites [14, 15]. However, the number of the graphene-related Ti composites is very limited on mechanical, wear and especially for thermal properties of Ti-GNPs composites. Up to now the published studies concentrated on the carbon black, carbon nanotubes (CNTs), carbon fiber and graphite-reinforced Ti composites. Li et al. reported the strength of the CNTs and graphite-reinforced Ti matrix. The tensile strength was developed the nearly 11% for 0.4 wt% CNTs/graphite ratio [16]. Kondoh et al. were reported the CNTs reinforced Ti composites. The highest yield, tensile strength and microhardness were evaluated as 697 MPa, 754 MPa, and 285 HV, respectively [17]. Threrujirapapong et al. developed the carbon black reinforced Ti composites. They reached up to 230 MPa tensile strength for low amount of carbon black [18]. Wang et al.

✉ Mevlüt Gürbüz
mgurbuz@omu.edu.tr

[1] Department of Mechanical Engineering, Faculty of Engineering, Ondokuz Mayıs University, 55139 Samsun, Turkey

[2] Department of Metallurgy and Materials Engineering, Ondokuz Mayıs University, 55139 Samsun, Turkey

[3] Vocational School, Metallurgy Program, Bilecik Seyh Edebali University, 11210 Bilecik, Turkey

[4] Biotechnology Application and Research Center, Bilecik Seyh Edebali University, 11210 Bilecik, Turkey

studied multiwall carbon nanotube reinforced Ti composites. They increased the compressive behavior of Ti composites from 685 to 1105 MPa [19]. After discovery of graphene in 2004, the graphene reinforced Ti composites rarely started to be reported. Using of graphene in Ti matrix 96% increase in nano-hardness and 16% increase in elastic modulus were reported by Zhang et al. [20]. Nearly 54% higher tensile strength for 0.1 wt% Gr was published by Zhang et al. [21]. Graphene reinforced Ti composites and their strength enhanced up to 915 MPa by Chen et al. [22]. In our previous paper, we studied the effect of the process parameters such as sintering temperature, time and graphene content on microhardness of the Ti composites. The optimum sintering temperature, time and graphene amount were reported as 1150 °C, 120 min and 0.15 wt% GNPs [23]. Moreover, the investigation of thermal conductivity for metal-matrix composites has great attention in various potential applications such as defense, aviation and automotive [24, 25]. Sabori et al. [26] reported the 0.5–1.0 wt% GNPs added aluminum matrix composites which had lower thermal conductivity with GNPs content and temperature. Yang et al. [27] studied the thermal conductivity of graphene added Ti composites at room temperature. It reduces with increasing the GNPs ratio. As given few studies were published about thermal behavior of GNPs reinforced metal composites which are limited.

As mentioned, few considerable studies have been presented and the number of published studies are not enough to understand the effect of the graphene on properties. Because they focused just process parameters and general mechanical properties of Ti composites. To our knowledge, there is no detailed publication, especially on wear and thermal properties of graphene reinforced Ti composites instead of mechanical behavior.

The present study focuses on the effect of GNPs concentration on tensile/compressive strength, wear-resistance and thermal conductivity of the Ti matrix composite which was fabricated by the powder metallurgy method.

2 Experimental Procedure

In this study Ti powder (Alfa Aesar, − 325 mesh) was used as a matrix material with a purity of 99.5%. GNPs (Grafen Chemical Industries Co.) is used as a reinforced material that has a specific surface area of 120–150 m^2/g, 5–10 µm diameter and thickness of 5–10 nm. The theoretical density of Ti powder and GNPs are approximately 4.5 g/cm^3 and 2.25 g/cm^3, respectively.

As given Fig. 1, the powder metallurgy method was used to produce the Ti-GNPs composites. First of all, ultrasonic homogenization has been applied to provide a good

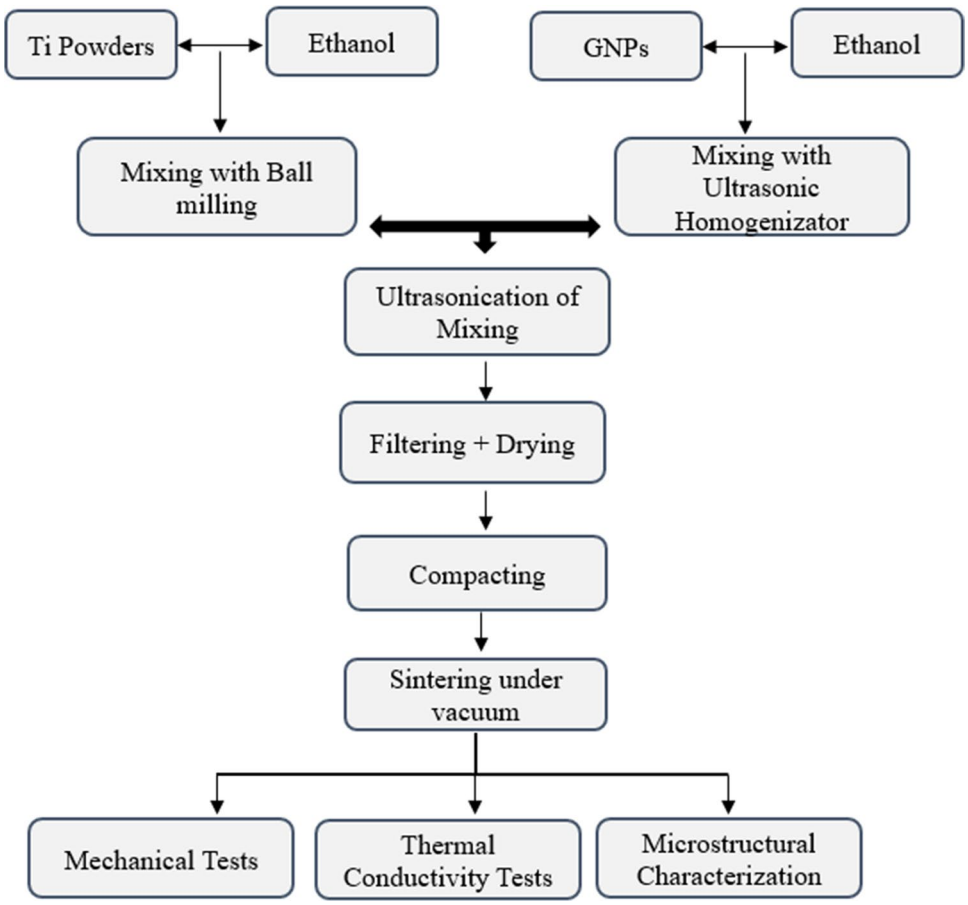

Fig. 1 Schematic diagram of Ti-GNPs composite fabrication with the PM method

dispersion of graphene. Ti and GNPs in different proportions (0.15, 0.30, 0.45, 0.60 wt%) were mixed with ethanol in the ball mill and then filtration and drying steps were applied. The dried powders were pressed in a die at 900 MPa. As a final step, the composite green samples were sintered in a tube furnace under a vacuum and inert atmosphere. The sintering conditions for sintering temperature ($T = 1100$ °C) and sintering time ($t = 120$ min) were determined in our previous paper [23].

The scanning electron microscopy with energy dispersive X-ray component (SEM, Jeol JSM-7001F) was used to evaluate the microstructure and elemental map analyses of composites. The crystal structure of powder and composites were performed with X-ray diffraction analysis (XRD, Rigaku Smartlab). Compressive and tensile properties were tested by Instron 5982-100 kN test machine. The sizes of the density, hardness, and compressive test specimens were nearly Ø10 × 20 mm. Also, the sizes of the tensile test specimens with rectangular cross-section were approximately 200 mm × 20 mm × 20 mm. The wear properties of pure Ti and Ti-GNPs composites were performed with the pin-on-disc method for 10–20–30 N. The stainless steel disc 2379 cold work tool steel was used as the counterpart. The sliding velocity and distance were selected as 200 rpm and 500 m.

3 Results and Discussion

3.1 Characterisation of Raw and Composite Materials

Figure 2a, b gives the SEM images of Ti and GNPs powders. The morphology of Ti has sharp-edged particles (Fig. 2a). GNPs consist of a few layers of two-dimensionally arranged graphene nanosheets (Fig. 2b). In Fig. 2c, the average Ti particle size is nearly 45 µm.

XRD patterns of Ti, GNPs powder and Ti-GNPs composites are given in Fig. 3a–c. From XRD analysis, it is clear that Ti powder peaks are presented at $2\theta = 29°$, 37°, 41°, 53°, 63°, 71°, 76°. Moreover, GNPs' peak is expected at $2\theta = 26.5°$. The XRD analyses of sintered GNPs reinforced Ti composites are shown in Fig. 3c. The XRD patterns do not include the graphene diffraction due to the low amount of GNPs and the low detection limit of XRD. Also, titanium carbide (TiC) peaks up to 0.45 wt% GNPs are not detected. However, the in situ TiC phase is formed with increasing GNPs.

Figure 4a–d presents the SEM image and elemental distribution of Ti and carbon (C) from GNPs for Ti-0.15 wt% GNPs composite after sintering at 1100 °C for 120 min. The titanium-rich region is seen with red color and the carbon-rich region with green color in EDX map analysis. From this

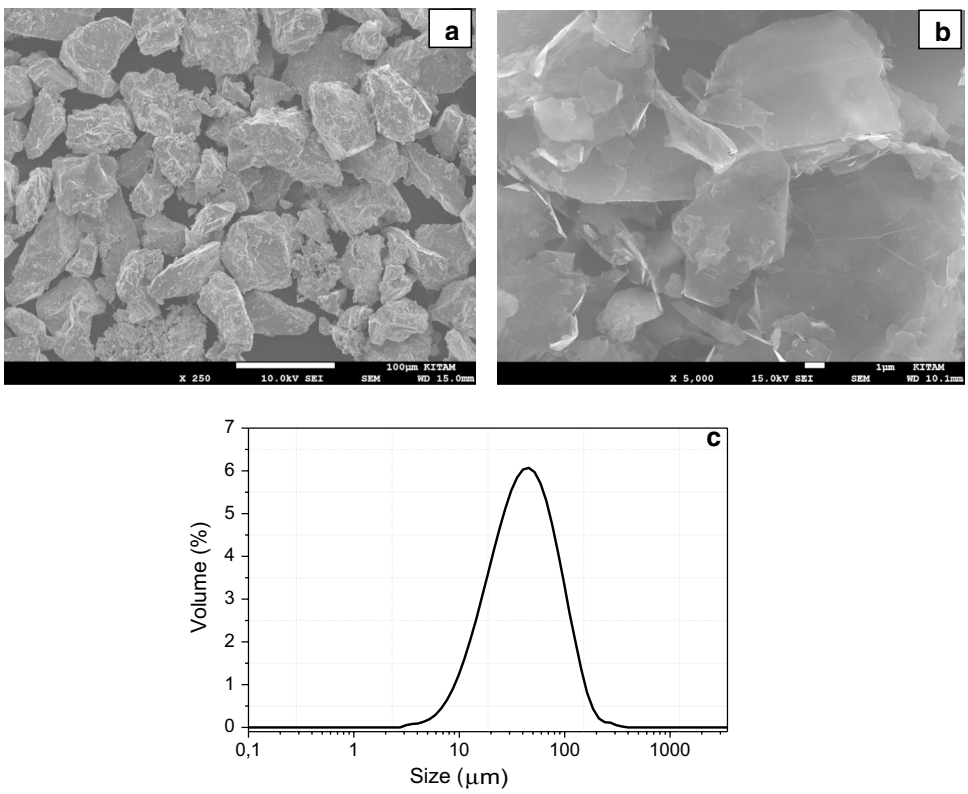

Fig. 2 SEM images of Ti, GNPs powder (**a**, **b**) and particle size distribution of Ti powder (**c**)

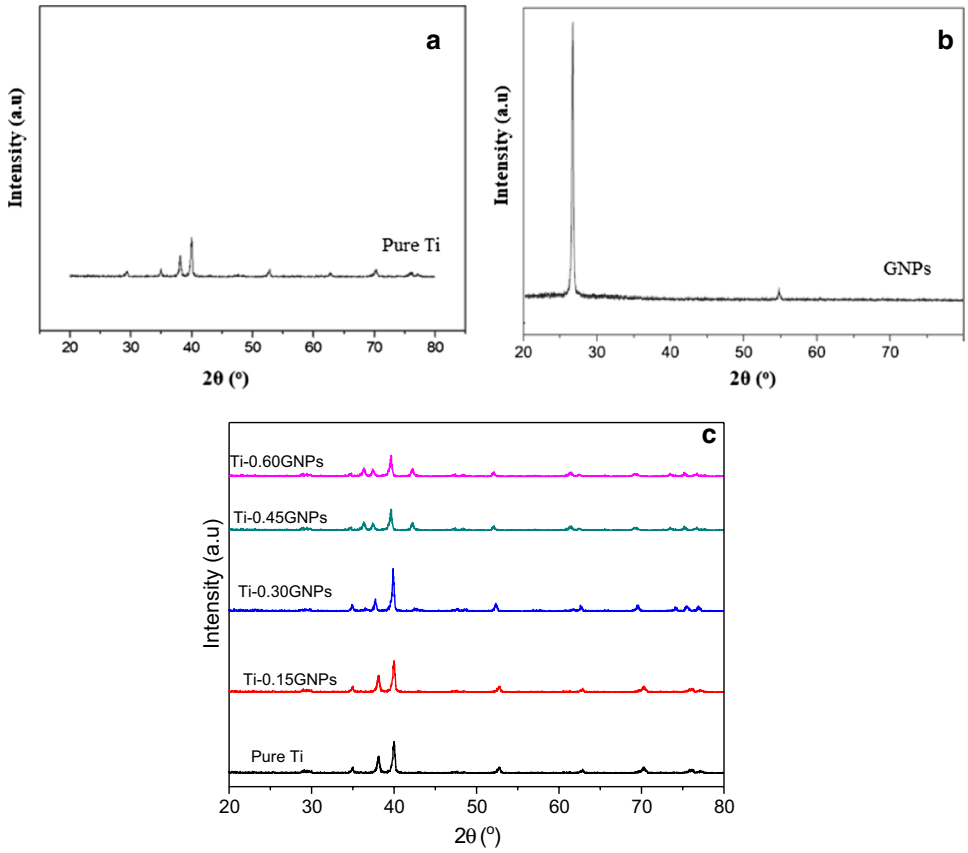

Fig. 3 XRD patterns of Ti, GNPs powders (**a**, **b**) and fabricated Ti-GNPs composites (**c**)

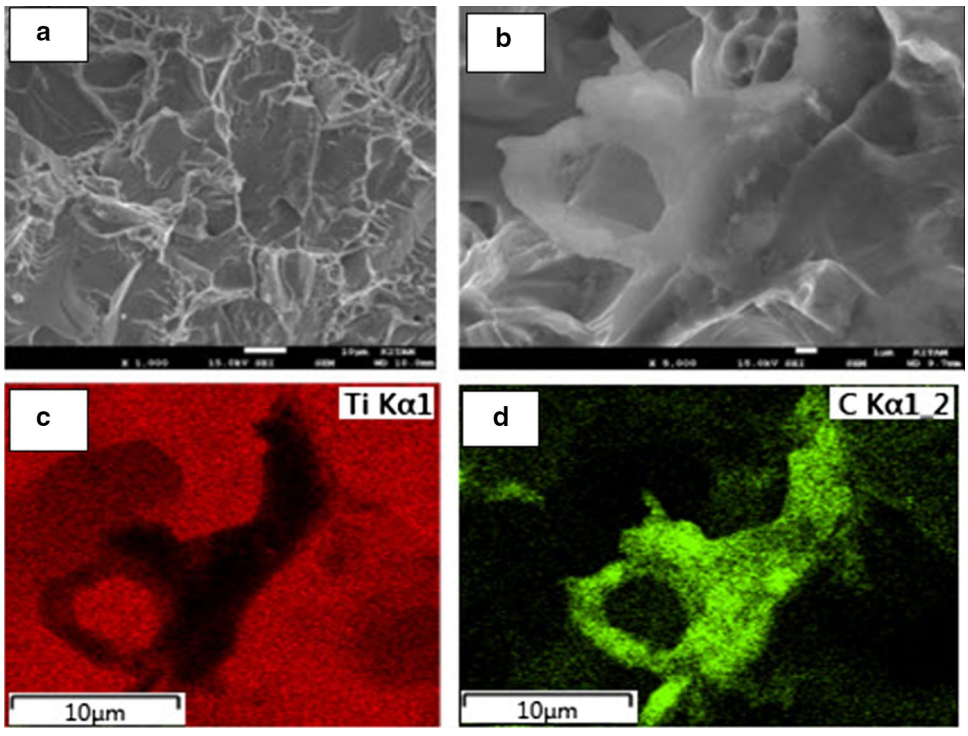

Fig. 4 SEM image of Ti-0.15 GNPs composite (**a**, **b**), elemental distribution of Ti (**c**) and C from GNPs(**d**). (Color figure online)

analysis, the uniform carbon distributions from GNPs in Ti matrix can be clearly seen.

3.2 Compressive and Tensile Behavior of Composites

Figure 5a, b gives the compressive and tensile behavior of GNPs reinforced composites for various graphene content (0.15, 0.30, 0.45 and 0.60 wt%). The highest ultimate compressive strength obtained with 0.15 wt% GNPs (845 MPa) and the other results are 0.30 wt% (800 MPa), 0.45 wt% (689 MPa), 0.60 wt% (649 MPa), respectively. The addition of 0.45, 0.60 wt% GNPs reduced the compressive strength of titanium matrix composites. Figure 5b shows that the ultimate tensile stress of pure Ti is 413 MPa and the ultimate tensile stress of Ti-0.15 GNPs composite is 613 MPa. As addition of graphene to the titanium, the tensile stress increased by 48.4%. It was observed that the ultimate tensile stress decreased to 425 MPa with increasing graphene (Ti-0.60 GNPs). The results are still higher than pure Ti. Graphene has been shown to increase the mechanical properties of the composite. It has been seen in previous studies that ultimate tensile strength increases and the ductility decreases as the amount of graphene additive increases [28, 29]. As given figures, both compressive and tensile strength is enhanced for the low content of graphene. The possible explanation is that the development of composite mechanical properties with GNPs is related to load transfer, thermal expansion coefficient mismatch and Orowan looping. The low amount of homogenously distributed GNPs acts as 2D obstacles at Ti grain boundaries. It led to prevent grain growth during sintering. These homogeneous distributed GNPs act as a barrier to the dislocation movement which causes the increase of dislocation density and dislocation strengthening. The dislocation strengthening is known as dislocation density mechanisms. The enhancement of the dislocation density controls the mechanical properties of the composites due to the nanosize structure and plate-like shape of the GNPs. Also, the thermal expansion coefficient mismatch between matrix and reinforcement elements causes the production of dislocation at the interphase. This led to increasing mechanical properties. Moreover, Orowan looping is another mechanism to understand the mechanical properties. The GNPs particles in Ti matrix creates the production of residual dislocation loops around the reinforcement materials. These fabricated loops develop higher mechanical properties [30, 31]. On the other hand, the compressive and tensile strength of Ti composites decreased with increasing GNPs content due to the agglomeration of GNPs and easy sliding during plastic deformation. GNPs act as a good solid-lubricant during compaction and tensile test for higher GNPs content. It causes less friction between the particles. Therefore, the solid-lubricant effect of GNPs facilitates the sliding under plastic deformation [32, 33].

3.3 Wear Behavior of Composites

Wear tests were performed on graphene additive titanium composites to investigate the wear behavior of composites, mass loss, wear loss between particles should be determined by using the pin-on-disc wear test unit (GUNT TM-260). In order to investigate the tribological behaviours of the sintered samples, pin-on-disc tests under dry conditions were conducted. The counterpart disc material was made of stainless steel 65 HRC. A counterpart disc diameter of 20 mm made of hard-faced stainless steel was used. First, the sliding

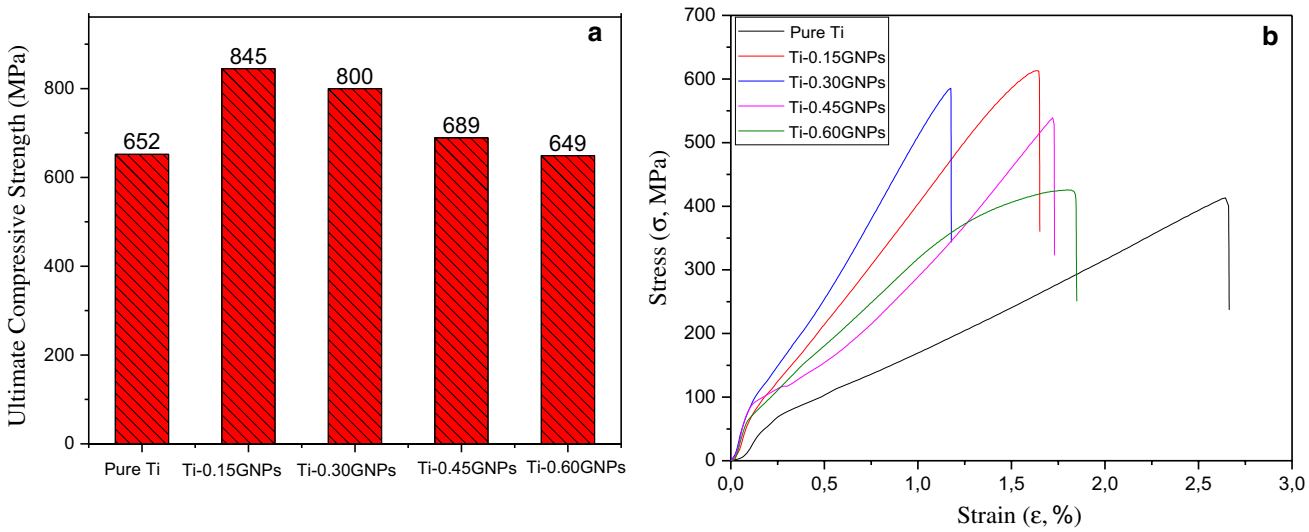

Fig. 5 The variation of the ultimate compressive and tensile strength (**a**, **b**) for various GNPs content. (Color figure online)

distance (L) can be calculated in order to detect the wear rate as given in Eq. 1.

$$L = 2\pi r \times n \times t \quad (1)$$

where r is the radius of counterpart disc (20 mm), n is the number of revolutions (200 rpm), t is the testing time (20 min), and L is the sliding distance (500 m). The tests were performed at different loads (10 N, 20 N, 30 N). The volume of worn material (ΔV) can be calculated by Eq. 2. And also the wear rate (WR) of composites can be calculated as presented in Eq. 3 [34].

$$\Delta V = \frac{\Delta m}{\rho} \quad (2)$$

$$WR = \frac{\Delta V}{F \times L} \quad (3)$$

where Δm is the mass loss ρ is the density of GNPs-Ti composite. WR is the wear rate (mm^3/Nm) and F is the applied load (N).

As load in the wear test increased, mass loss and wear rate of Ti-GNPs composites increased as expected. In Fig. 6a, b, the lowest mass loss ($\Delta m = 0.6$ mg) and wear rate ($WR = 286 \times 10^{-5}$ mm^3/Nm) are performed for Ti-0.15GNPs when evaluated under 10 N. As GNPs additive increases, wear rate (Ti-0.60 GNPs, $WR = 7.2 \times 10^{-5}$ mm^3/Nm) is deteriorated. When the graphene is used as a reinforcement, it tends to agglomerate which can be low and high sized with GNPs content. The larger sized GNPs agglomeration causes the inhomogeneous distribution and more damaged surfaces.

After the wear test, all worn surfaces were analyzed by SEM. In Fig. 7a–c, SEM micrographs present the worn surfaces of pure Ti, Ti-0.15GNPs and Ti-0.60GNPs composites under 10 N. The pure Ti and Ti-0.60 GNPs include great damage on the wear surfaces. Ti-0.15 GNPs composite has a significantly much better surface than other samples due to more uniform particle distributions in Ti without agglomeration for low GNPs content. However, the wear properties are deteriorated with increasing GNPs content which led to agglomeration. These agglomerated reinforcement particles distributed locally which causes to increasing wear rate.

3.4 Thermal Behavior of Composites

Figure 8a–c gives the thermal behavior of Ti-GNPs composites depending on graphene content and temperature. Thermal diffusivity and conductivity of composites increased up to 0.30 wt% graphene content. This is thought to be a result of the homogeneous distribution of graphene. It is seen that the increase rate of the thermal diffusivity and conductivity values maintain their value at high temperatures. As given in the Fig. 8 both diffusivity and conductivity are reduced with increasing temperature. It can be explained by phonon–phonon Umklapp scattering which decreases the diffusivity by reducing the mean free path in materials at high temperatures. The phonons provide the heat conduction through the Ti-GNPs composite at the GNPs-Ti interface. These interfaces act as a thermal barrier to heat flow it causes to the reduction of phonon mean free path [35, 36]. Moreover, intrinsic defects within the GNPs could lead to a barrier to thermal transport. The bend and twisted areas of GNPs at matrix grain boundaries can cause to a reduction in thermal conductivity by restricted the phonon free path [37]. Although there is a significant decrease in thermal properties over 0.30 wt% graphene. This can be explained due to the presence of porosity and low density agglomerated graphene in the matrix. As given Fig. 8d both stereo and SEM image confirm the presence of the porosity for higher content GNPs. Optimal dispersion of graphene is important

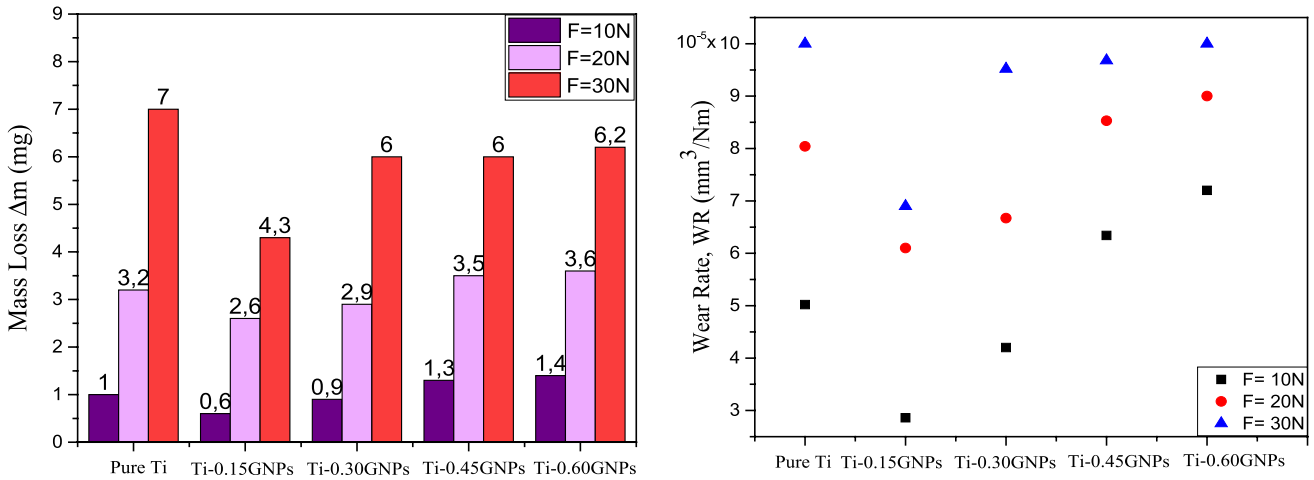

Fig. 6 The variation of mass loss (**a**) wear rate (**b**) of Ti-GNPs composites

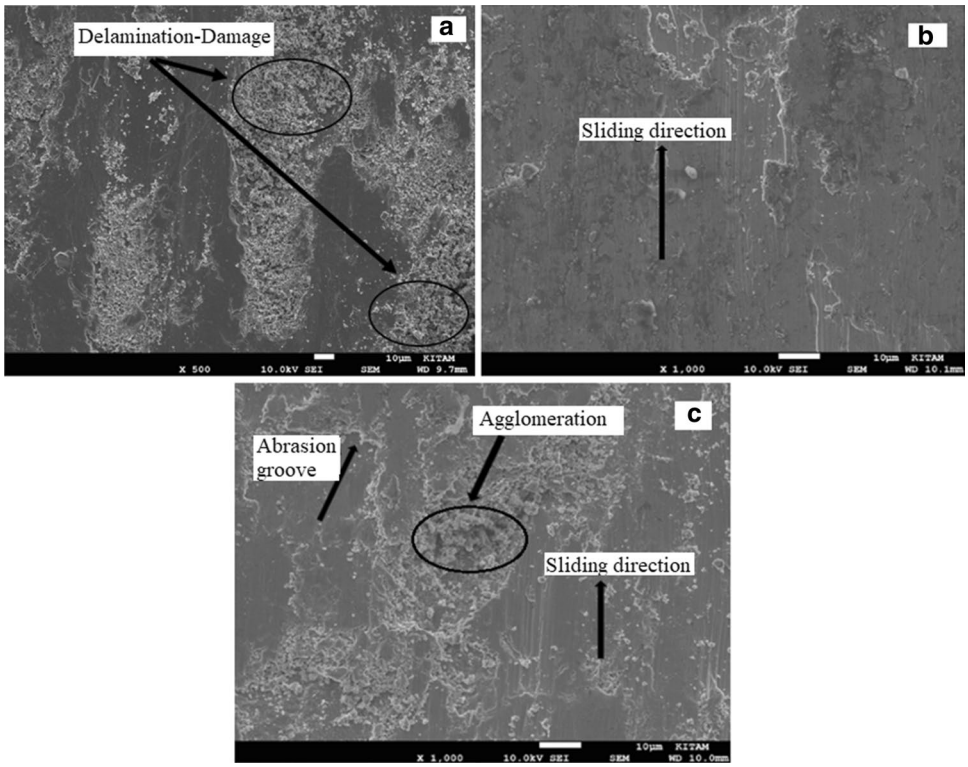

Fig. 7 SEM micrographs of worn surface: pure Ti (**a**), Ti-0.15GNPs (**b**), Ti-0.60GNPs (**c**)

for thermal diffusivity since there is a percolation threshold in spherical systems. Thermal diffusivity is the heat flow rate in non-stationary conditions, and these graphene agglomerates act as barriers, preventing heat dissipation [38].

4 Conclusion

In this study 0.15, 0.30, 0.45, 0.60 wt% GNPs reinforced Ti composites were successfully fabricated by the PM method. The effect of the GNPs content on the tensile, compressive strength, wear and thermal behavior of the Ti composites were investigated in detail. A significant increase in mentioned properties was observed with small amount of GNPs addition (0.15 wt%). The highest compressive strength (845 MPa) and tensile strength (613 MPa) were observed for the Ti-0.15GNPs composite compared with pure Ti compressive strength (652 MPa) and tensile strength (413 MPa). The lowest mass loss (0.6 mg for 10 N), and lowest wear rate ($WR = 2.86 \times 10^{-5}$ mm^3/Nm for 10 N) were obtained at Ti-0.15 GNPs compared with pure titanium (nearly 1 mg mass loss and $WR = 5 \times 10^{-5}$ mm^3/Nm). The highest thermal conductivity (16 W/mK) and diffusivity (7.1 mm^2/s) were tested for Ti-0.30 GNPs c^{o}mposites at room temperature. The thermal properties were decreased with increasing graphene content and temperature. It summaries that, graphene is a good candidate to enhance the mechanical, wear and thermal behavior of Ti composites.

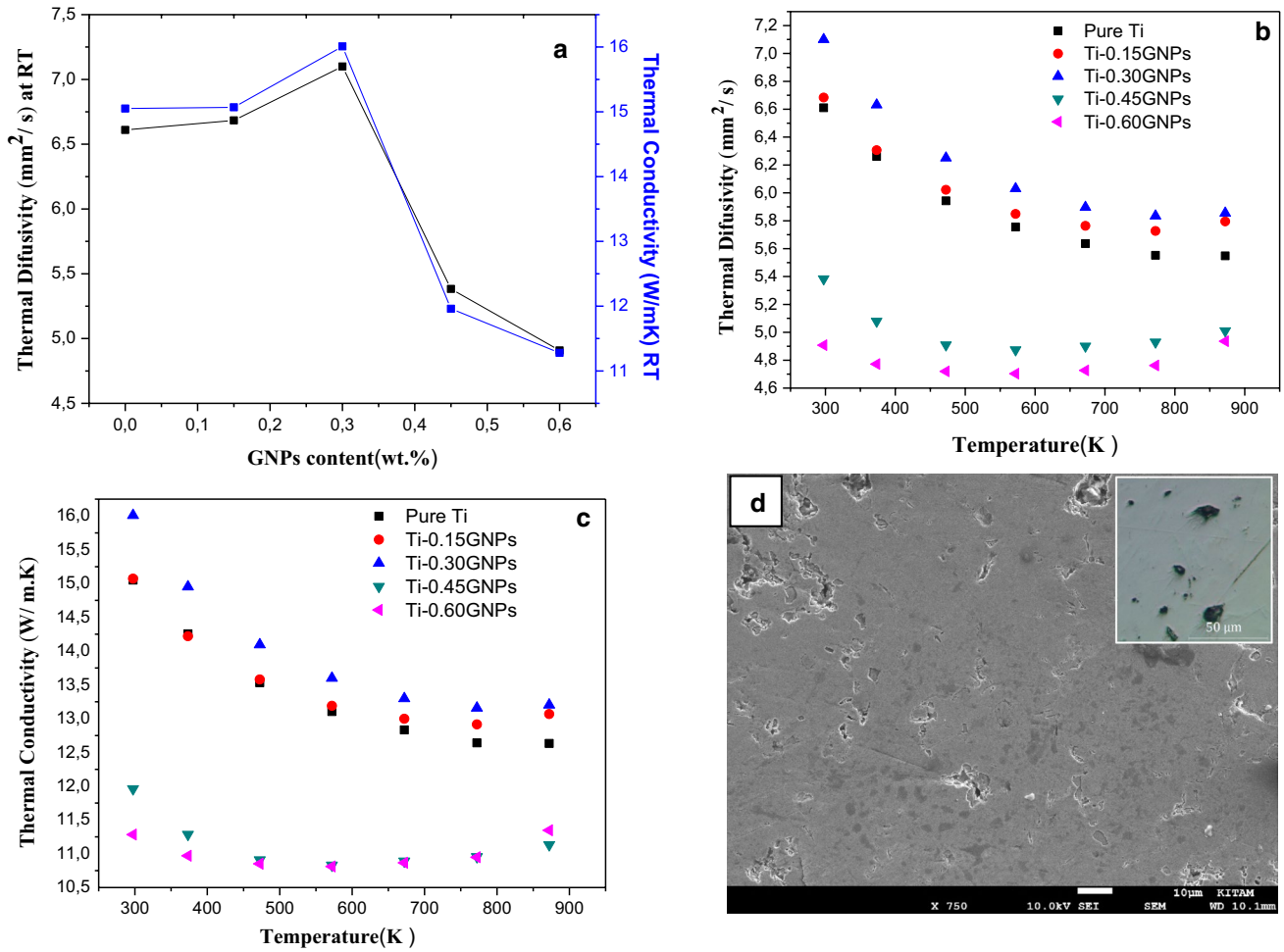

Fig. 8 Thermal diffusivity (**a**, **b**), conductivity of Ti-GNPs depend on graphene content and temperature (**c**), stereo and SEM images of the Ti polished surface for 0.30 wt% graphene (**d**)

Acknowledgements We would like to special thanks to The Scientific and Technological Research Council of Turkey (TUBITAK) (Project No: 217M154) and Ondokuz Mayıs University, Scientific Research Project Department under the grants (PYO.MUH.1902.15.001 and PYO.MUH.1906.14.006). In addition, we would like to thanks to Bilecik Şeyh Edebali University Scientific Research Foundation for supported (Project No: 2019-01.BŞEÜ0.11-01, 2019).

References

1. M. Vakili-Azghandi, M. Roknian, J.A. Szpunar, S.M. Mousavizade, Surface modification of pure titanium via friction stir processing: microstructure evolution and dry sliding wear performance. J. Alloy. Compd. **816**, 152557 (2020)
2. N. Joy, S. Prakash, A. Krishnamoorty, A. Antony, Experimental investigation and analysis of drilling in Grade 5 Titanium alloy (Ti-6Al-4 V). Mater. Today Proc. **21**, 335–339 (2020)
3. N. Li, C. Cui, S. Liu, L. Zhao, S. Liu, Fabrication of the Ti_5Si_3/Ti composite inoculants and its refining mechanism on pure titanium. Met. Mater. Int. **23**(2), 397–404 (2017)
4. Y. Kim, P. Yadav, J. Hahn, X. Xiao, D.B. Lee, Oxidation of titanium matrix composites reinforced with (TiB + TiC) particulates. Met. Mater. Int. **25**, 627–632 (2019)
5. D.E. Alman, J.A. Hawk, The abrasive wear of sintered titanium matrix-ceramic particle reinforced composites. Wear **225–229**, 629–639 (1999)
6. F.M. Kgoete, A.P.I. Popoola, O.S.I. Fayomi, Influence of spark plasma sintering on microstructure and corrosion behaviour of Ti-6Al-4V alloy reinforced with micron-sized Si_3N_4 powder. Def. Technol. **14**(5), 403–407 (2018)
7. E.P. Randviir, D.A.C. Brownson, C.E. Banks, A decade of graphene research: production, applications and outlook. Mater. Today **17**(9), 426–432 (2014)
8. V. Singh, D. Joung, L. Zhai, S. Das, S.I. Khondaker, S. Seal, Graphene based materials: past, present and future. Prog. Mater. Sci. **56**(8), 1179–1271 (2011)
9. M.E. Turan, H. Zengin, Y. Sun, Dry sliding wear behavior of (MWCNT + GNPs) reinforced AZ91 magnesium matrix hybrid

composites. Mater. Int. (2019). https://doi.org/10.1007/s12540-019-00338-8
10. M. Hedayatian, K. Vahedi, A. Nezamabadi, A. Momeni, Microstructural and mechanical behavior of Al6061-graphene oxide nanocomposites. Mater. Int. (2019). https://doi.org/10.1007/s12540-019-00361-9
11. D.M. Chen, P.M. Shenai, Y. Zhao, Tight binding description on the band gap opening of pyrene-dispersed graphene. Phys. Chem. Chem. Phys. **4**, 1515–1520 (2013)
12. A.H. Castro Neto, F. Guinea, N.M.R. Peres, K.S. Novoselov, A.K. Geim, Rev. Mod. Phys. **81**(1), 109–162 (2009)
13. Y. Zhu, S. Murali, W. Cai, X. Li, J.W. Suk, J.R. Potts, R.S. Ruoff, Graphene and graphene oxide: synthesis, properties, and applications. Adv. Mater. **22**(35), 3906–3924 (2010)
14. J. Wang, Z. Li, G. Fan, H. Pan, Z. Chen, D. Zhang, Reinforcement with graphene nanosheets in aluminium matrix composites. Scr. Mater. **66**(8), 594–597 (2012)
15. L. Chen, H. Konishi, A. Fehrenbacher, C. Ma, J. Xu, H. Choi, H. Xu, F.E. Pfefferkorn, X. Li, Novel nanoprocessing route for bulk graphene nanoplatelets reinforced metal matrix nanocomposites. Scr. Mater. **67**(1), 29–32 (2012)
16. S. Li, B. Sun, H. Imai, T. Mimoto, K. Kondoh, Powder metallurgy titanium metal matrix composites reinforced with carbon nanotubes and graphite. Compos. Part A Appl. Sci. **48**, 57–66 (2013)
17. K. Kondoh, T. Threrujirapapong, H. Imai, J. Umeda, B. Fugetsu, Characteristics of powder metallurgy pure titanium matrix composite reinforced with multi-wall carbon nanotubes. Compos. Sci. Technol. **69**(7–8), 1077–1081 (2009)
18. T. Threrujirapapong, K. Kondoh, H. Imai, J. Umeda, B. Fugetsu, Mechanical properties of a titanium matrix composite reinforced with low cost carbon black via powder metallurgy processing. Mater. Trans. **50**, 2757–2762 (2009)
19. F. Wang, Z. Zhang, Y. Sun, Y. Liu, Z. Hu, H. Wang, A.V. Korznikov, E. Korznikova, Z. Liu, S. Osamu, Rapid and low temperature spark plasma sintering synthesis of novel carbon nanotube reinforced titanium matrix composites. Carbon **95**, 396–407 (2015)
20. X.N. Mu, H.N. Cai, H.M. Zhang, Q.B. Fan, F.C. Wang, Z.H. Zhang, Y. Wu, Y.X. Ge, S. Chang, R. Shi, Y. Zhou, D.D. Wang, Uniform dispersion of multi-layer graphene reinforced pure titanium matrixcomposites viaflake powder metallurgy. Mater. Sci. Eng. A Struct. **725**, 541–548 (2018)
21. Y. Song, Y. Chen, W.W. Liu, W.L. Li, Y.G. Wang, D. Zhao, X.B. Liu, Microscopic mechanical properties of titanium composites containing multi-layer graphene nanofillers. Mater. Des. **109**, 256–263 (2016)
22. X.N. Mu, H.M. Zhang, H.N. Cai, Q.B. Fan, Z.H. Zhang, Y. Wu, Z.J. Fu, D.H. Yu, Microstructure evolution and superior tensile properties of low content graphene nanoplatelets reinforced pure Ti matrix composites. Mater. Sci. Eng. A Struct. **687**, 164–174 (2017)
23. T. Mutuk, M. Gürbüz, Effect of process parameters on hardness and microstructure of graphene reinforced titanium composites. J. Compos. Mater. **52**(4), 543–551 (2017)
24. A. Kelly, Composites for the 1990s. Philos. Trans. R. Soc. **322**, 409–423 (1987)
25. G.R. Sharp, T.A. Loftin, *Applications of high thermal conductivity composites to electronicsand spacecraft thermal design, Report, Tech Memo 102434* (National Aeronautics and Space Administration, Washington, DC, 1990)
26. A. Saboori, M. Pavese, C. Badini, P. Fino, Microstructure and thermal conductivity of Al-graphene composites fabricated by powder metallurgy and hot rolling Techniques. Acta Met. Sin. (Engl. Lett.) **30**(7), 675–687 (2017)
27. W. Yang, W. Huang, Z. Wang, F. Shang, W. Huang, B. Zhang, Thermal and mechanical properties of graphene–titanium composites synthesized by microwave sintering. Acta Met. Sin. (Engl. Lett.) (2016). https://doi.org/10.1007/s40195-016-0445-7
28. Z. Cao, X. Wang, J. Li, Y. Wu, H. Zhang, J. Guo, S. Wang, Reinforcement with graphene nanoflakes in titanium matrix composites. J. Alloy Compd. **696**, 498–502 (2017)
29. M. Rashad, F. Pan, A. Tang, Y. Lu, M. Asif, S. Hussain, J. She, J. Gou, J. Mao, Effect of of graphene nanoplatelets (GNPs) addition on strength and ductility of magnesium–titanium alloys. J. Magnes. Alloys **1**(3), 242–248 (2013)
30. M. Rashad, F. Pan, H. Hu, M. Asif, S. Hussain, J. She, Enhanced tensile properties of magnesium composites reinforced with graphene nanoplatelets. Mater. Sci. Eng. A Struct. **630**, 36–44 (2015)
31. F.H. Latief, E.M. Sherif, Effects of sintering temperature and graphite addition on the mechanical properties of aluminum. J. Ind. Eng. Chem. **18**(6), 2129–2134 (2012)
32. S.F. Bartolucci, J. Paras, M.A. Refiee, J. Refiee, S. Lee, D. Kapoor, N. Koratkar, Graphene–aluminum nanocomposites. Mater. Sci. Eng. A Struct. **532**(27), 7933–7937 (2011)
33. J. Wozniak, M. Kostecki, T. Cygan, M. Buczek, A. Olszyna, Self-lubricating aluminium matrix composites reinforced with 2D crystals. Compos. Part B Eng. **111**, 1–9 (2017)
34. H. Attar, K.G. Prashanth, A.K. Chaubey, M. Calin, L.C. Zhang, S. Scudino, J. Eckert, Comparison of wear properties of commercially pure titanium prepared by selective laser melting and casting processes. Mater. Lett. **142**, 38–41 (2015)
35. A.A. Balandin, Thermal properties of graphene, carbon nanotubes and nanostructured carbon materials. Nat. Mater. **10**, 569–581 (2011)
36. L. Kuamri, T. Zhang, G.H. Du, W.Z. Li, Q.W. Wang, A. Datye, K.H. Wu, Thermal properties of CNT-alumina nanocomposites. Compos. Sci. Technol. **68**(9), 2178–2183 (2008)
37. P. Miranzo, E. Garcia, C. Ramirez, J. Gonzalez-Julian, M. Belmonte, M.I. Osendi, Anisotropic thermal conductivity of silicon nitride ceramics containing carbon nanostructures. J. Eur. Ceram. Soc. **32**(8), 1847–1854 (2012)
38. M. Selvakumar, T. Ramkumar, P. Chandrasekar, Thermal characterization of titanium–titanium boride composites. J. Therm. Anal. Calorim. **136**(1), 419–424 (2019)